



Onset of Benard–Marangoni Convection in a Composite Layer with Anisotropic Porous Material

Y. H. Gangadharaiah

Department of Mathematics, New Horizon College of Engineering, Bangalore-560 103, India

Email: gangu.honnappa@gmail.com

(Received January 18, 2013; accepted October 7, 2015)

ABSTRACT

The effects of thermal anisotropy and mechanical anisotropy on the onset of Bernard-Marangoni convection in composite layers with anisotropic porous material is studied. The upper fluid surface, free to atmosphere is considered to be deformable. The eigen value problem is solved using a regular perturbation technique with wave number a as perturbation parameter. It is observed that both stabilizing and destabilizing factors can be enhanced thermal anisotropic parameter and mechanical anisotropic parameter so that a more precise control (suppress or augment) of thermal convective instability in a layer of fluid or porous medium is possible.

Key words: Bernard-marangoni convection; Mechanical anisotropy; Thermal anisotropy.

NOMENCLATURE

| | | | |
|--------|-------------------------------|-----------|--|
| A | ratio of heat capacity | Pr | Prandtl number for fluid layer |
| D | differential operator | Pr_m | porous medium Prandtl number |
| d | thickness of the fluid layer | R | Rayleigh number in the fluid layer |
| d_m | thickness of the porous layer | R_m | Rayleigh number in a porous medium |
| Da | Darcy number | T | temperature |
| h | heat transfer coefficient | T_0 | temperature at the interface |
| M | Marangoni number | W | amplitude of perturbed vertical velocity |
| l, m | wave number in x and y | \vec{V} | velocity vector (u, v, w) |
| p | pressure | | |

1. INTRODUCTION

Convection within a two-layer system constructed by a layer of fluid overlying a porous material saturated with the same fluid has numerous geophysical and industrial applications, such as the manufacturing of composite materials used in the aircraft and automobile industries, flow of water under the Earth's surface, flow of oil in underground reservoirs and growing of compound films in thermal chemical vapour deposition reactors. A detailed review is given by Nield & Bejan (2006), with current highly relevant literature including Straughan (2001; 2008); Carr (2004); Chang (2004; 2005; 2006); Shivakumara *et al.* (2006; 2012); Suma *et al.* 2012; and Hill and Straughan (2009).

The onset of pure Rayleigh convection in the superposed liquid-porous layers, sandwiched by

two horizontal infinite rigid and thermal conductive wall, heated from below Beavers and Joseph (1967). The Darcy's law is applied together with the experimentally suggested slip condition proposed by Beavers and Joseph (1967) at the liquid-porous interface. They indicate that the neutral instability curves for the onset of instability is bimodal which possess two local minima. The key parameter is the ratio between the depth of liquid layer and that of porous layer. Its critical value $h_c = 0.13$, below which the instability is called the long-wave mode, and above which the instability is called the short-wave mode. After their work, several (Hill and Straughan 2009; Gangadharaiah 2013 and Pearson (1958) studied the coupled gravity and surface tension driven instability problems in a similar system, and all focused on the depth ratio as the crucial parameter which can determine the mode of convection.

Nield (1977) has investigated the linear stability problem of superposed fluid and porous layers with buoyancy and surface tension effects at the deformable upper free surface by using the Beavers–Joseph slip condition at the interface. The thermal stability for different systems of superposed porous and fluid regions has also been analyzed by Taslim and Narusawa(1989). Chen (1990) has implemented a linear stability analysis to investigate the effect of throughflow on the onset of thermal convection in a fluid layer overlying a porous layer with an idea of understanding the control of convective instability by the adjustment of throughflow. McKay(1988) has considered the onset of buoyancy-driven convection in superposed reacting fluid and porous layers. Nield (1988) has argued about the modelling of Marangoni convection in a fluid saturated porous medium and has suggested the consideration of composite porous–fluid layer system in analyzing the problem. Khalili *et al.* (2001) have obtained the closed form solution for Chen’s model by considering the upper and lower boundaries are insulating to temperature perturbations.

In all the above superposed fluid and porous layers problems, the porous medium is considered to be isotropic. Castinel and Combarous (1975) were the first to study both experimentally and theoretically the onset of convection in a layer of porous medium with anisotropic permeability. The onset of buoyancy-driven convection due to heating from below in a system consisting of a fluid layer overlying a porous layer with anisotropic permeability and thermal diffusivity has been discussed by Chen *et al.*(1990). Recently, Shivakumara *et al.* (2011) have investigated the criterion for the onset of surface tension-driven convection in the presence of temperature gradients in a two-layer system comprising a fluid saturated anisotropic porous layer over which lies a layer of fluid while the effect of internal heating on the problem has been considered by Shivakumara *et al.* (2012).

The aim of the present paper is, therefore, to study convective instability in a composite system solely due to temperature dependent surface tension effects at the upper deformable free surface of a fluid layer overlying an anisotropic porous layer. The effect of surface deformation on the onset of Bernard-Marangoni convection and both mechanical and thermal anisotropy is considered by simplifying it to a horizontally isotropic case. Such a model is of physical relevance to practical situations since many porous structures display anisotropy where the permeability and in turn the thermal conductivity in the vertical direction is different to that in the horizontal plane. A modified Darcy equation is employed to describe the flow regime in the anisotropic porous medium and at the interface of porous and fluid media the Beavers-Joseph classical slip condition is used. The boundaries are considered to be insulated to temperature perturbations. A regular perturbation technique with wave number as a perturbation parameter is used to solve the eigen value problem

in a closed form. A wide-ranging parametric study is undertaken to explore their impact on the stability characteristics of the system.

2. FORMULATION OF THE PROBLEM

We consider a incompressible fluid-saturated horizontal anisotropic porous layer of thickness d_m underlying a fluid layer of thickness d , the lower boundary of the anisotropic porous layer is taken to be rigid, while the upper surface has a deflection $\Omega(x, y, t)$ from mean (see Fig.1).

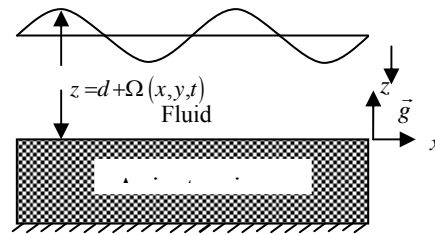


Fig. 1. Physical model.

The lower hot rigid boundary $z_m = -d_m$, is kept at a constant temperature T_h , while upper surface $z = d$ is free to atmosphere of constant temperature T_h . A Cartesian coordinate system (x, y, z) is chosen such that the origin is at the interface between the fluid layer and the anisotropic porous layer and the z -axis is vertically upward. The surface tension σ is assumed to vary linearly with temperature in the form $\sigma = \sigma_0 - \sigma_T (T - T_0)$, where σ_0 is the constant reference value.

The governing equations for the fluid and porous layer are:

Fluid layer:

$$\nabla \cdot \vec{V} = 0 \tag{1}$$

$$\rho_0 \left(\frac{\partial \vec{V}}{\partial t} + (\vec{V} \cdot \nabla) \vec{V} \right) = -\nabla p + \rho_0 \vec{g} [1 - \alpha(T - T_0)] + \mu \nabla^2 \vec{V} \tag{2}$$

$$\frac{\partial T}{\partial t} + (\vec{V} \cdot \nabla) T = \kappa \nabla^2 T \tag{3}$$

Porous layer:

$$\nabla_m \cdot \vec{V}_m = 0 \tag{4}$$

$$\frac{\rho_0}{\phi} \frac{\partial \vec{V}_m}{\partial t} = -\nabla_m p_m - \mu K^{-1} \cdot \vec{V}_m + \rho_0 \vec{g} [1 - \alpha(T_m - T_0)] \tag{5}$$

$$A \frac{\partial T_m}{\partial t} + (\vec{V}_m \cdot \nabla_m) T_m = \nabla_m \cdot (\kappa_m \cdot \nabla_m T_m) \tag{6}$$

Here \vec{V} is the velocity vector, p is the pressure, g is the gravitational acceleration, T is the

temperature, while \vec{V}_m , p_m , T_m are the corresponding quantities in the porous layer, κ is the thermal diffusivity, μ is the fluid viscosity, ϕ is the porosity of the porous medium, A is the ratio of heat capacities, ρ_0 is the fluid density, \underline{K} is the permeability tensor and $\underline{\kappa}_m$ is the thermal diffusivity tensor. The permeability and thermal diffusivity tensors of the porous medium are assumed to be constants and have principal axis aligned with the coordinate system so that $\underline{K}^{-1} = K_x^{-1}\hat{i}\hat{i} + K_y^{-1}\hat{j}\hat{j} + K_v^{-1}\hat{k}\hat{k}$ and $\underline{\kappa}_m = \kappa_{mx}\hat{i}\hat{i} + \kappa_{my}\hat{j}\hat{j} + \kappa_{mv}\hat{k}\hat{k}$. We restrict to horizontal isotropic porous media and consider $K_x = K_y (=K_h)$ and $\kappa_{mx} = \kappa_{my} (= \kappa_{mh})$. It may be noted that the permeability and effective thermal diffusivity in the horizontal and vertical directions in an anisotropic porous layer are denoted by K_h, κ_{mh} and K_v, κ_{mv} , respectively.

The boundary conditions are

At the lower rigid boundary, $z_m = -d_m$,

$$q_m = 0, \quad T = T_h$$

At the deformable free surface

$$\frac{\partial \Omega}{\partial t} + u \frac{\partial \Omega}{\partial x} + v \frac{\partial \Omega}{\partial y} = w, \quad k_i \nabla T \cdot \hat{n} + HT = 0$$

$$2\mu d_m = \frac{\partial \sigma}{\partial T} \nabla T \cdot \hat{n}, \quad p_a - p + 2\mu d_m = \sigma \nabla \cdot \hat{n}.$$

In order to investigate the stability of the basic solution, infinitesimal disturbances are introduced in the form

$$\vec{V} = \vec{V}', \quad T = T_b(z) + T', \quad p = p_b(z) + p'$$

$$\vec{V}_m = \vec{V}'_m, \quad T_m = T_{mb}(z) + T'_m, \quad p_m = p_{mb}(z) + p'_m$$

where the primed quantities are the perturbations and assumed to be small. Substitute these equations in Eqs. (1)–(6) and linearized in the usual manner.

The pressure term is eliminated from Eqs. (2) and (5) by taking curl twice on these two equations and only the vertical component is retained. The variables are then nondimensionalized using $d, d^2/\kappa, \kappa/d$ and $T_0 - T_u$ as the units of length, time, velocity, and temperature in the fluid layer and $d_m, d_m^2/\kappa_{mv}, \kappa_{mv}/d_m$ and $T_l - T_0$ as the corresponding characteristic quantities in the porous layer. Note that separate length scales are chosen for the two layers so that each layer is of unit depth. In this manner, the detailed flow fields in both the fluid and porous layers can be clearly discerned for all depth ratios $\zeta = d/d_m$ and

Then performing a normal mode expansion of the dependent variables in both fluid and porous layers as

$$(w, T, \Omega) = [W(z), \Theta(z), Z] f(x, y) \quad (7)$$

$$(w_m, T_m) = [W_m(z_m), \Theta_m(z_m)] f_m(x_m, y_m) \quad (8)$$

Where $f(x, y)$ and $f_m(x_m, y_m)$ are horizontal plan forms satisfying $\nabla_h^2 f = -a^2 f$ and $\nabla_{mh}^2 f_m = -a_m^2 f_m$. Here a and a_m are the horizontal wave numbers in fluid and porous layer respectively. For matching the solutions in two layers to be possible, we should have $a/d = a_m/d_m$, and hence $\zeta = a/a_m$. we obtain the following ordinary differential equations: S

$$(D^2 - a^2)^2 W = a^2 R \Theta \quad (9)$$

$$(D^2 - a^2) \Theta = -W \quad (10)$$

$$\left[\left(\frac{1}{\xi} \right) D_m^2 - a_m^2 \right] W_m = -a_m^2 R_m \Theta_m \quad (11)$$

$$(D_m^2 - \eta a_m^2) \Theta_m = -W_m \quad (12)$$

where D and D_m denote differentiation with respect to z and z_m respectively, $a = \sqrt{l^2 + m^2}$ and $a_m = \sqrt{\tilde{l}^2 + \tilde{m}^2}$ are correspondingly the overall horizontal wave numbers in the fluid and porous layers.

The boundary conditions are

$$W = D\Theta + B_i(\Theta - Z) = 0 \quad \text{at } z = 1 \quad (13)$$

$$D^2 W + Ma^2(\Theta - Z) = 0 \quad \text{at } z = 1 \quad (14)$$

$$Cr(D^2 - 3a^2)DW - (B_0 + a^2)a^2 Z = 0 \quad \text{at } z = 1 \quad (15)$$

$$W_m = D_m \Theta_m = 0 \quad \text{at } z_m = -1 \quad (16)$$

and those at the interface (i.e $z = 0$) are

$$W = \frac{\zeta}{\varepsilon_T} W_m \quad (17)$$

$$D\Theta = D_m \Theta_m \quad (18)$$

$$\Theta = \frac{\varepsilon_T}{\zeta} \Theta_m \quad (19)$$

$$\left[D^2 - 3a^2 \right] DW = \frac{-\zeta^4}{Da\varepsilon_T \xi} D_m W_m \quad (20)$$

$$\left[D^2 - \frac{\beta\zeta}{\sqrt{Da\xi}} D \right] W = \frac{-\beta\zeta^3}{\varepsilon_T \sqrt{Da\xi}} D_m W_m \quad (21)$$

3. METHOD OF SOLUTION

For the assumed boundary conditions the eigen

value problem is solved by using regular perturbation technique with wave number a as a perturbation parameter. The dependent variables in both the fluid and porous layers are now expanded in powers of a^2 in the form

$$(W, \Theta) = \sum_{i=0}^N (a^2)^i (W_i, \Theta_i) \quad (22)$$

$$(W_m, \Theta_m) = \sum_{i=0}^N \left(\frac{a^2}{\zeta^2} \right)^i (W_{mi}, \Theta_{mi}) \quad (23)$$

Substitution of Eqs(22) and (23) into Eqs. (9)–(12) and the boundary conditions (13)–(21) yields a sequence of equations for the unknown functions $W_i(z), \Theta_i(z), W_{mi}(z)$ and $\Theta_{mi}(z)$ for $i = 0, 1, 2, \dots$

At the leading order in a^2 Eqs. (9)–(12) become, respectively,

$$D^4 W_0 = 0 \quad (24)$$

$$D^2 \Theta_0 = -W_0 \quad (25)$$

$$D_m^2 W_{m0} = 0 \quad (26)$$

$$D_m^2 \Theta_{m0} = -W_{m0} \quad (27)$$

and the boundary conditions (13)–(21) become

$$W_{m0} = 0, \quad D_m \Theta_{m0} = 0 \text{ at } z_m = -1 \quad (28)$$

$$W_0 = 0, \quad D \Theta_0 = 0, \quad D^2 W_0 = 0 \text{ at } z = 1 \quad (29)$$

And at the interface (*i. e* $z = 0$)

$$W_0 = \frac{\zeta}{\varepsilon_T} W_{m0} \quad (30)$$

$$\Theta_0 = \frac{\varepsilon_T}{\zeta} \Theta_{m0} \quad (31)$$

$$D \Theta_0 = D_m \Theta_{m0} \quad (32)$$

$$D^2 W_0 - \frac{\beta \zeta}{\sqrt{Da \zeta}} D W_0 = \frac{-\beta \zeta^3}{\varepsilon_T \sqrt{Da \zeta}} D_m W_{m0} \quad (33)$$

$$D^3 W_0 = \frac{-\zeta^4}{\varepsilon_T Da \zeta} D_m W_{m0} \quad (34)$$

The solution to the zeroth order equations is given by

$$W_0 = 0, \quad \Theta_0 = \frac{\varepsilon_T}{\zeta} \quad (35)$$

$$W_{m0} = 0, \quad \Theta_{m0} = 1 \quad (36)$$

At the first order in a^2 , Eqs(9)–(12) then reduce to

$$D^4 W_1 = R \frac{\varepsilon_T}{\zeta} \quad (37)$$

$$D^2 \Theta_1 - \frac{\varepsilon_T}{\zeta} = -W_1 \quad (38)$$

$$D_m^2 W_{m1} = -\xi R_m \quad (39)$$

$$D_m^2 \Theta_{m1} - \eta = -W_{m1} \quad (40)$$

and the boundary conditions (13)–(21) become

$$W_{m1} = 0, \quad D_m \Theta_{m1} = 0 \text{ at } z_m = -1 \quad (41)$$

$$W_1 = 0, \quad D \Theta_1 = 0 \text{ at } z = 1 \quad (42)$$

$$D^2 W_1 + M \left(\frac{\varepsilon_T}{\zeta} - Z_0 \right) = D^3 W_1 - \frac{B_0}{Cr} Z_0 = 0 \text{ at } z = 1 \quad (43)$$

And at the interface (*i. e* $z = 0$)

$$W_1 = \frac{1}{\zeta \varepsilon_T} W_{m1} \quad (44)$$

$$\Theta_1 = \frac{\varepsilon_T}{\zeta^3} \Theta_{m1} \quad (45)$$

$$D \Theta_1 = \frac{1}{\zeta^2} D_m \Theta_{m1} \quad (46)$$

$$D^2 W_1 - \frac{\beta \zeta}{\sqrt{Da \zeta}} D W_1 = \frac{-\beta \zeta}{\varepsilon_T \sqrt{Da \zeta}} D_m W_{m1} \quad (47)$$

$$D^3 W_1 = \frac{-\zeta^2}{\varepsilon_T Da \zeta} D_m W_{m1}. \quad (48)$$

Integrating Eq. (38) between $z = 0$ and 1, and Eq. (40) between $z_m = -1$ and 0, using the relevant boundary conditions and adding the resulting equations, we obtain the following solvability condition:

$$\int_0^1 W_1 dz + \frac{1}{\zeta^2} \int_{-1}^0 W_{m1} dz = \frac{\varepsilon_T}{\zeta} + \frac{\eta}{\zeta^2} \quad (49)$$

The general solution of Eqs. (37) and (39) are respectively given by

$$W_1 = R \left[c_1 + c_2 z + c_3 z^2 + c_4 z^3 + \frac{\varepsilon_T z^4}{24 \zeta} \right] \quad (50)$$

$$W_{m1} = R \left[c_5 + c_6 z_m - \frac{Da \xi \varepsilon_T^2}{2 \zeta^4} z_m^2 \right] \quad (51)$$

Substituting for W_1 and W_{m1} from Eqs. (49) and performing the integration, we obtain an expression for the critical Rayleigh number R_C in the form

$$R_m^c = \frac{(3DaB_0\beta(\varepsilon_T \zeta(1-\zeta) + \xi \eta \zeta(1-\zeta)))}{\Delta_1 + \Delta_2} \quad (52)$$

4. RESULTS AND DISCUSSION

The stability analysis of Bernard-Marangoni convection in a two-layer system consisting of a fluid layer overlying an anisotropic porous layer investigated theoretically. The resulting eigen value problem is solved using a regular perturbation technique with wave number as a perturbation parameter.

First we will discuss Rayleigh-Benard convection (in the absence of Marangoni number $M = 0$) and the results are presented for The results are presented for $\sqrt{Da} = 3.04 \times 10^{-3}$ (which correspond to 3-cm-deep porous layer consisting of 3-mm-diameter glass beads (Chen1990) $B_o = 0.1$, $\varepsilon_T = 0.725, \beta = 1$ and $Cr = 0$ the range of depth ratio $\zeta = 10^{-4}$ approximating pure porous layer case to $\zeta = 1$ (two layers of equal depth). The case $\zeta = 10^{-4}$ corresponding to a porous layer with an extremely thin overlying fluid layer, Fig. 2 shown, R_m^c increase with the decreasing ξ . Physically, this means that the conduction solution in the porous medium becomes more stable and the critical wavelength decreases as the horizontal permeability decreases. Smaller horizontal permeability inhibits horizontal motion, and the conduction solution is thus stabilized. The larger resistance to horizontal flow also leads to a shortening of the horizontal wavelength at onset. In the same figure, it is seen that for a given & smaller values of the horizontal thermal diffusivity correspond to destabilization of the basic state, and the onset of convection at a smaller wavelength, This can be explained by the fact that, as η decreases, a heated fluid parcel loses less heat in the horizontal directions, and hence retains its buoyancy better. Therefore, the base state becomes less stable, and the wavelength is reduced.

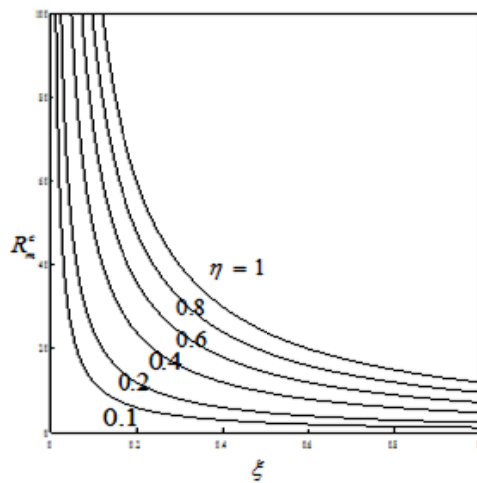


Fig. 2. Variation of R_m^c with ξ for different values of η when $\zeta = 10^{-4}$

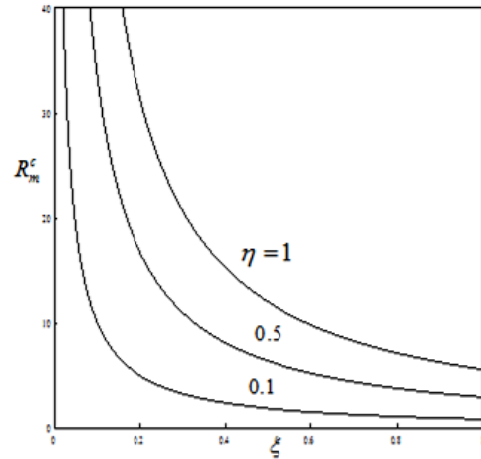


Fig. 2. a Variation of R_m^c with ξ for different values of η when $\zeta = 0.1$.

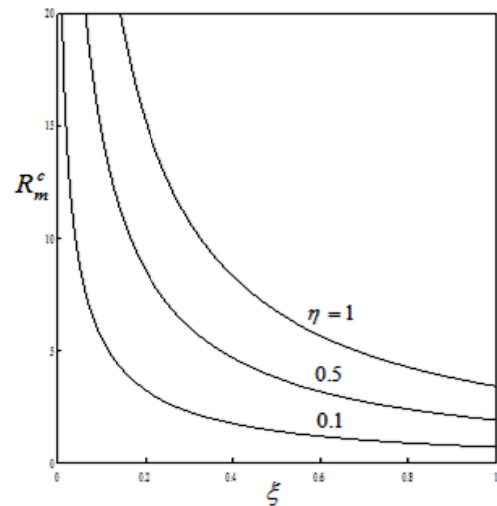


Fig. 3. Variation of R_m^c with ξ for different values of η when $\zeta = 0.2$.

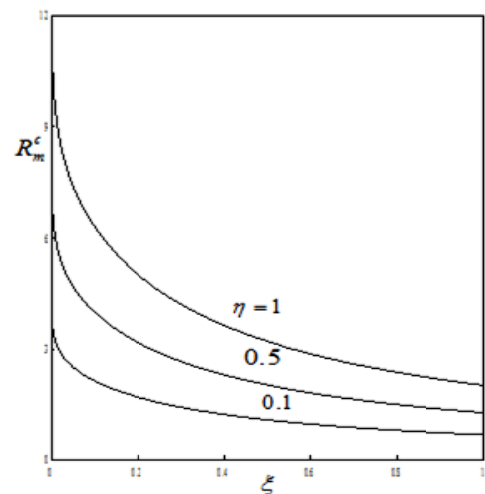


Fig. 4. Variation of R_m^c with ξ for different values of η when $\zeta = 0.5$.

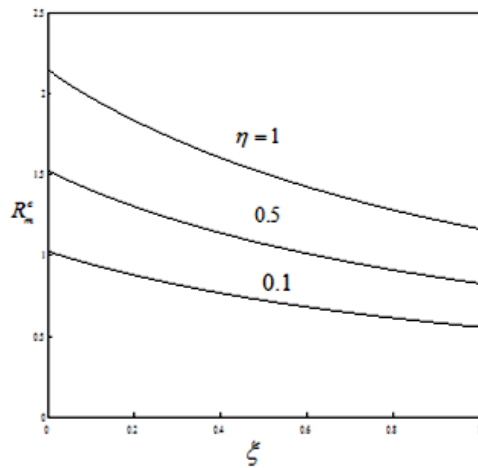


Fig. 5. Variation of R_m^c with ξ for different values of η when $\zeta = 1$.

Table 1 Critical values of Rayleigh number R_m^c with different values of ζ , η and ξ

| ξ | η | R_m^c | | | |
|-------|--------|---------------|---------------|---------------|-------------|
| | | $\zeta = 0.1$ | $\zeta = 0.2$ | $\zeta = 0.5$ | $\zeta = 1$ |
| 0.1 | 0.1 | 10.026 | 5.554 | 2.138 | 0.946 |
| 0.2 | | 5.061 | 3.257 | 1.702 | 0.878 |
| 0.4 | | 2.455 | 1.778 | 1.234 | 0.767 |
| 0.6 | | 1.585 | 1.214 | 0.973 | 0.681 |
| 0.8 | | 1.158 | 0.917 | 0.805 | 0.612 |
| 1.0 | | 0.905 | 0.735 | 0.686 | 0.556 |
| 0.1 | 0.5 | 33.375 | 14.624 | 3.987 | 1.405 |
| 0.2 | | 16.793 | 8.574 | 3.174 | 1.304 |
| 0.4 | | 8.149 | 4.681 | 2.502 | 1.139 |
| 0.6 | | 5.266 | 3.196 | 1.816 | 1.012 |
| 0.8 | | 3.8451 | 2.416 | 1.501 | 0.910 |
| 1.0 | | 3.005 | 1.935 | 1.280 | 0.826 |
| 0.1 | 1.0 | 62.524 | 25.960 | 6.298 | 1.979 |
| 0.2 | | 31.460 | 15.222 | 5.014 | 1.836 |
| 0.4 | | 15.267 | 8.309 | 3.637 | 1.604 |
| 0.6 | | 9.866 | 5.675 | 2.868 | 1.425 |
| 0.8 | | 7.203 | 4.288 | 2.376 | 1.281 |
| 1.0 | | 5.630 | 3.436 | 2.02 | 1.164 |

For depth ratios $\zeta = 0.1, 0.2, 0.5, 1.0$ we have computed R_m^c for three values of η , over a range of ξ . The results are shown in Figs2a- 5, the behaviour of R_m^c is similar to that of above case $\zeta = 10^{-4}$ presented in Fig.2. The critical values of R_m^c for different values of ζ , ξ and η are tabulated in Table 1 since our main interest is to look at the dramatic effects of mechanical, and thermal anisotropic parameter on the onset of Rayleigh-Benard convection. From the Table it is seen that (i) increasing value of ξ , R_m^c decreases monotonically as the value of ζ increases, (ii) increasing value of η , R_m^c decreases monotonically as the value of ζ increases and (iii) increasing η is to delay the onset of Rayleigh-Benard convection

and (iv) the higher value of ζ the porous layer behaves like an essentially solid layer, the influence of the permeability anisotropy is less significant than that of the thermal diffusivity.

In the absence of thermal buoyancy (i.e. $R = 0$) we merely consider the Marangoni convective instability at the upper free surface. The critical Marangoni number computed for different values of Da and ζ when $\varepsilon_T = 0.725$, $\beta = 1$, $\xi = 0.5$, $Cr = 0$ and $\eta = 0.5$ are tabulated in Table 2. The results of Shivakumara *et al.* (2011) are also exhibited in the Table for the sake of comparison. It is seen that our results are in good agreement with those of Shivakumara *et al.* (2011) in the absence of thermal buoyancy (i.e. $R = 0$). Figure 6 shows that M_c as a function of ζ for different values of Crispation number Cr (i.e., influence of surface tension) for fixed values of $Da = 4 \times 10^{-6}$, $B_o = 0.1$, $\varepsilon_T = 0.725$, $\beta = 1$, $R = 0$,

$\xi = 0.5 = \eta$ and $B_i = 0$ (Since we are dealing with layers of small thickness, the value of B_i does not appreciably affect the results for $B_i = 0$, Takashima(1981). From figure, it may be noted that an increase in value of Cr is to decrease the value of M_c and thus making system more unstable. The reason being that an increase in Cr is to increase the deflection of the upper free surface, which in turn, promotes instability much faster. It is also seen that for a fixed value of $Cr (\leq 10^{-3})$, M_c increases initially with ζ reaches a peak value, and then starts decreasing before attaining an asymptotic value with further increase in ζ (see Fig.6). But this trend goes on diminishing with an increase in the value of Cr value of $Cr = 0.1$, M_c remains almost invariant with ζ .

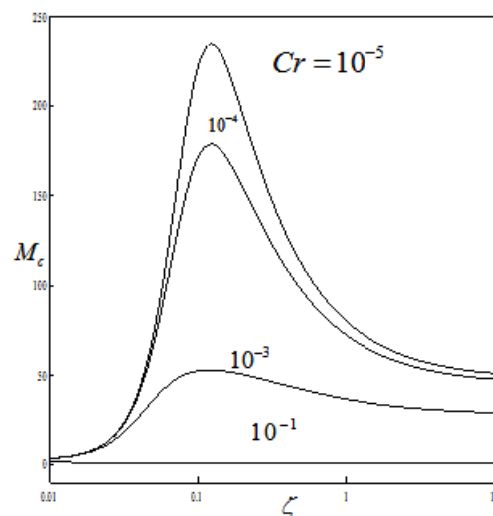


Fig. 6. Variation of M_c with ζ for different values of Cr when $\xi = 0.5 = \eta$, $\varepsilon_T = 0.725$

Table 2 Critical Marangoni number for different values of depth ratio and Darcy number when $Bi = 0, B_o = 0.1, R = 0$ and $\eta = 0.5 = \xi$

| ζ | Shiva kumara (2011) $M_c (Bi = 0)$ | | | | Present study $M_c (Bi = 0)$ | | | |
|---------|---------------------------------------|--------|--------|--------|---------------------------------|--------|--------|--------|
| | Da | | | | Da | | | |
| | 0.001 | 0.003 | 0.005 | 0.007 | 0.001 | 0.003 | 0.005 | 0.005 |
| 0.1 | 5.178 | 3.198 | 2.631 | 2.324 | 5.176 | 3.196 | 2.642 | 2.333 |
| 0.5 | 68.934 | 42.717 | 31.999 | 26.042 | 68.956 | 42.721 | 31.983 | 26.040 |
| 1.0 | 72.414 | 64.118 | 58.314 | 53.799 | 72.423 | 64.123 | 58.323 | 53.789 |
| 1.5 | 66.136 | 62.651 | 60.069 | 57.917 | 66.121 | 62.648 | 60.066 | 57.927 |
| 2.0 | 62.091 | 60.058 | 58.567 | 57.317 | 62.089 | 60.065 | 58.572 | 57.307 |
| 2.5 | 59.465 | 58.055 | 57.038 | 56.190 | 59.471 | 58.062 | 57.044 | 56.196 |

Table 3 Critical values of Marangoni number M_c with different values of η and ξ for

$$Da = 4 \times 10^{-6}, B_o = 0.1$$

| ξ | M_c with $\eta = 0.5$ | | | η | M_c with $\xi = 0.5$ | | |
|-------|-------------------------|----------------|----------------|--------|------------------------|----------------|----------------|
| | $Cr = 10^{-6}$ | $Cr = 10^{-4}$ | $Cr = 10^{-2}$ | | $Cr = 10^{-6}$ | $Cr = 10^{-4}$ | $Cr = 10^{-2}$ |
| 0.1 | 80.850 | 72.118 | 36.5709 | 0.1 | 64.3399 | 50.287 | 29.9701 |
| 0.5 | 80.654 | 72.038 | 36.5465 | 0.5 | 80.6547 | 72.038 | 36.5465 |
| 1.0 | 80.505 | 71.924 | 36.5274 | 1.0 | 111.5191 | 97.162 | 42.0645 |
| 1.5 | 80.389 | 71.834 | 36.5124 | 1.5 | 146.351 | 120.253 | 45.8783 |
| 2.0 | 80.290 | 71.758 | 36.4994 | 2.0 | 179.151 | 141.574 | 48.6718 |

The critical values of M_c for different values of ξ , η and Cr are tabulated in Table 3 when $Da = 4 \times 10^{-6}, B_o = 0.1, \varepsilon_T = 0.725, \zeta = 1, R = 0$ and $\beta = 1$ since our main interest is to look at the dramatic effects of mechanical anisotropy parameter ξ and thermal anisotropy parameter η . It is noted that M_c attains higher values at lower values of ξ and Cr . That is, decrease in the mechanical anisotropy parameter is to delay the onset of Marangoni convection. This is because, decrease in ξ corresponds to smaller horizontal permeability which in turn hinders the motion of fluid in the horizontal direction. As a consequence, the conduction process in the porous medium becomes as observed more stable and hence higher values of M_c are needed for the onset of Marangoni convection. To the contrary, in the same Table it is observed that decreasing η is to hasten the onset of Marangoni convection. This may be attributed to the fact that the decrease in η amounts to decrease in the horizontal thermal diffusivity. Thus heat cannot be transported through the porous layer and hence the horizontal temperature variations in the fluid required to sustain convection

are less efficiently dissipated for small η . Hence, the base state becomes less stable leading to lower values of critical Marangoni number.

The variation of M_c obtained as a function of depth ratio ζ for different values of Da when $B_i = 0, \varepsilon_T = 0.725, \beta = 1, Cr = 0.001$ and $\xi = 0.5 = \eta$ are presented in a Fig.7. As expected, the effect of decrease in Da is to increase the critical Marangoni number. Furthermore, the variation in ζ has a significant effect on the onset of convection for the values of $\zeta \leq 0.2$, while the curves of different Da merge in to one when $\zeta > 0.2$.

5. CONCLUSION

The stability analysis of Bernard-Marangoni convection in a two-layer system consisting of a fluid layer overlying a anisotropic porous layer investigated theoretically. It is observed that the mechanical and thermal anisotropy parameters influence the stability of the system significantly. Increasing the mechanical anisotropy parameter has a destabilizing effect on the system, while an opposite trend is noticed with an increase in the

value of thermal anisotropy parameter. And decreasing the Crispation number leads to stabilization of the system and the increasing slip parameter is to delay the onset of Bernard-Marangoni convection.. Thus, it is possible to either augment or suppress the onset of Bernard-Marangoni convection by suitably choosing the parametric values.

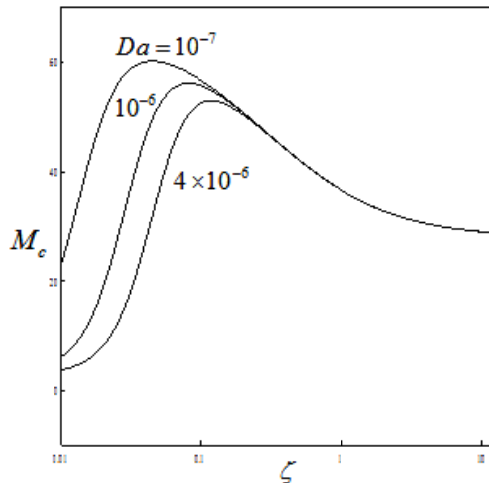


Fig.7. Variation of M_c with ζ for different values of Da when $\xi = 0.5 = \eta$, $\varepsilon_T = 0.725$.

ACKNOWLEDGMENTS

The author express their heartfelt thanks to the management of New Horizon College of Engineering, Bangalore for their encouragement.

REFERENCES

Carr, M. (2004). Penetrative convection in a superposed porous- medium–fluid layer via internal heating, *J. Fluid Mech.* 509, 305–329.

Chang, M. H. (2004). Stability of convection induced by selective absorption of radiation in a fluid overlying a porous layer, *Phys. Fluids.* 16, 3690–3698.

Chang, M. H. (2005). Thermal convection in superposed fluid and porous layers subjected to a horizontal plane couette flow, *Phys. Fluids.* 17, 064106-1–064106-7.

Chang, M. H. (2006). Thermal convection in superposed fluid and porous layers subjected to a plane Poiseuille flow, *Phys. Fluids.* 18, 035104-1–035104-10.

Chen, F. (1990). Throughflow effects on convective instability in superposed fluid and porous layers, *J. Fluid. Mech.* 231, 113–133.

Gangadharaiah, Y. H. (2013). Double-Diffusive Marangoni convection in a composite system. *International Journal of Innovative Research in Science, Engineering and Technology.* 131, 137-144.

Hill, A. A. and B. Straughan (2009). Poiseuille flow in a fluid overlying a highly porous material, *Adv. Water Resour.* 32, 1609-1614.

McKay, G. (1998). Onset of buoyancy-driven convection in superposed reacting fluid and porous Layers *J. Engg. Math.* 33, 31–46.

Nield, D. A. (1977). Onset of convection in a fluid layer overlying a layer of a porous medium, *J. Fluid Mech.* 81, 513–522.

Nield, D. A. and A. Bejan (2006). Convection in Porous Media. *Third. ed. Springer-Verlag.* New York.

Pearson, J. R. A. (1958). On convection cells induced by surface tension *J. Fluid Mech.* 4, 489–500.

Shivakumara, I. S., J. Lee, K. B. V. Chavaraddi (2011). Onset surface tension convection in a fluid layer overlying a layer of an anisotropic porous medium *Int. J. Heat Mass Transfer.* 54, 994-1001.

Shivakumara, I. S., S. P. Suma, R. Indira, and Y. H. Gangadharaiah (2012). Effect of internal heat generation on the onset of Marangoni convection in a fluid layer overlying a layer of an anisotropic porous medium. *Transp. Porous Med.* 92,727-743.

Shivakumara, I. S., S. P. Suma, and K. B. Chavaraddi (2006). Onset of surface-tension driven convection in superposed fluid and porous layers, *Arch. Mech.* 55, 327–348, 2006.

Straughan, B. (2001). Surface-tension-driven convection in a fluid overlying a porous layer, *Comput. Phys.* 170, 320–337.

Straughan, B. (2008). Stability and wave motion in porous media, *Appl. Math. Sci. Ser.vol.* 165. Springer, New York

Suma, S. P., Y. H. Gangadharaiah, R. Indira and I. S. Shivakumara (2012). Throughflow Effects on Penetrative Convection in Superposed Fluid and Porous Layers. *Transp. Porous Med.* 95, 91-110.

Takashima, M. (1981). Surface tension driven instability in a horizontal liquid layer with a deformable free surface. I. Stationary convection *Journal of the Physical Society of Japan.* 50, 2745–2750.

Takashima, M. (1981). Surface tension driven instability in a horizontal liquid layer with a deformable free surface. I. Stationary convection, *Journal of the Physical Society of Japan.* 50, 2745–2750.

Taslim, M. E. and V. Nurusawa (1989). Thermal stability of horizontally superposed porous and fluid layer, *ASME J. Heat Transf.* 111, 357-362.

